Engineering Science Aspects of the Hall-Petch Relation*

Ronald W. Armstrong
Center for Energetic Concepts Development
Department of Mechanical Engineering
University of Maryland
College Park, MD 21842, U.S.A.

ABSTRACT

Hall and Petch had established in the early 1950's a linear inverse square root of grain diameter dependence for yielding and cleavage of polycrystalline iron and steel materials, with ordinate intercept stress, σ_0, and slope value, k. Petch and colleagues extended the relationship in 1962 to the full stress – strain behavior of a diverse number of metals and alloys. Connection with other mechanical properties such as the hardness, fatigue and strain rate sensitivity properties was demonstrated in 1970. In 1983, Weng incorporated the dependence into a micromechanical analysis of material strength by building onto earlier Taylor-initiated work on multiply-coupled grain deformations. More recently, Armstrong, Weng and colleagues have applied dislocation and continuum mechanics models of the H-P relationship to predicting order-of-magnitude increases in strength properties of nanopolycrystalline materials, especially including description of the strain rate sensitivity dependence on average grain diameter. These topics are assessed from a dislocation mechanics viewpoint in the present report that provides H-P connection with the Taylor dislocation density based theory of strength properties, in $\sigma_{0\varepsilon}$, and with the Griffith brittle fracture theory by way of pointing to the H-P slope value, k_ε, being a microstructural stress intensity analogous to the fracture mechanics parameter, K.

1. Introduction

The present article is intended to honor the research accomplishments of George Weng in bringing together the Hall-Petch description of grain size dependent mechanical strength properties and the Taylor model of evaluating polycrystal strength properties through build-up of deformations among multiply-joined polycrystal grain orientations. Award of the Prager medal is especially deserved by Professor Weng because of Prager's interest too in the same subject of better understanding the deformation behaviors of polycrystalline materials. As will be seen in the present article, the relation of single crystal and polycrystalline strength properties was a major topic of research in the 20th century; and now in the 21st century constitutes a major effort directed toward producing nanopolycrystalline materials and measuring/understanding their mechanical properties. A Power Point presentation on the topic is listed [1] under "Publications" at the University of Maryland website http://www.cecd.umd.edu.

---

* Invited for George-Weng-honoring Prager Medal Symposium, 50th Annual Technical Meeting of the Society of Engineering Science, 28-31 July, 2013, Providence, RI.

2. Historical background

We begin a bit further back with 18th century historical reports provided first by Grignon [2], who noted that iron when it was fine-grained was better in its properties; and then by Reaumur [3], who noted that excellent steels were distinguished from mediocre ones by the fineness of their grains. The fineness of the grain structures was revealed by fracturing; see also Smith and Burke [4]. Grignon had proposed a decatetrahedral-hexagon shape for the morphology of individual crystal grains of iron while Smith has noted that Thomson, later to be Lord Kelvin, pointed in the 19th century to the 14-faced truncated octahedron known as a tetrakaidecahedron for the proposed polycrystal grain shape with minimum surface area per unit volume [5, 6].

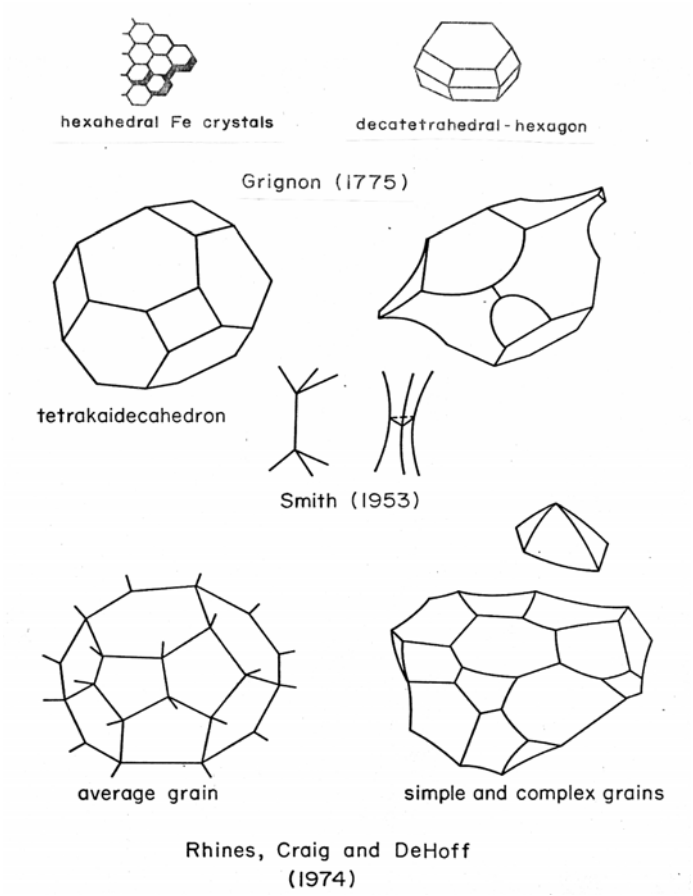

Figure 1. Historical and modern descriptions of grain shapes.

Figure 1 gives a schematic view of the grain constructions described by Grignon, Thomson and Smith. The curved surface modification of the tetrakaidecahedron shape and expansion of the boundary line had been suggested to Smith by Teller [6]. An average grain shape and examples of other real grain shapes had been described by Rhines, Craig and DeHoff [7] in a metallographic study of grain growth in aluminum. The line intercept method has the advantage of specifying the average material grain diameter independent of the shape of the grains.

Figure 2 is a schematic presentation of dislocation structures beginning from a pair of dislocations that might correspond to a dislocation density greater, say than 2 x 10^8 per cm^2 if the edge length of the crystal box were 1.0 micrometer in length per side [8]; then to a segmented slip band traversing a crystal grain to impinge on the encompassing grain boundary structure [9]; and lastly, to a model consideration proposed for first vestige of cleavage initiated in a sea of ductile fracturing by dislocation pile-ups blocked at a particle clump located within a grain boundary region [10]. The build-up of microstructure from a single dislocation to a slip band stress concentration within a single grain and then to critical grain/particle clump interaction within a pressure vessel steel has served previously as a basis for model developments proceeding onwards from the pioneering analyses of Hall and Petch [11].

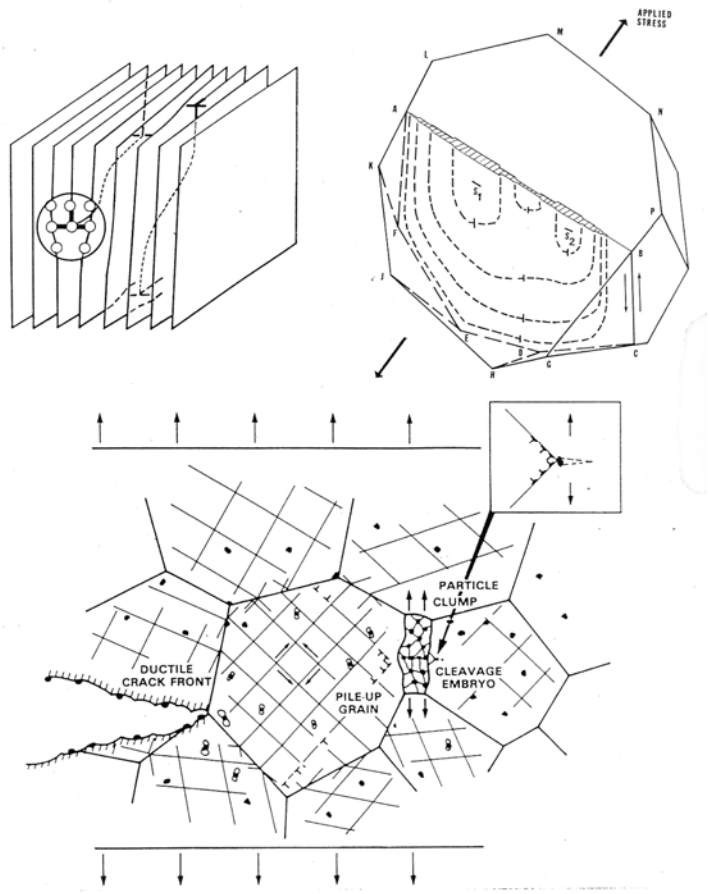

Figure 2. Schematic description of dislocation interactions at several structural levels.

3. Bcc *vs.* fcc deformation behaviors.

Figure 3 has been constructed from load - elongation results employed by Unwin at the end of the 19th century to differentiate between body-centered cubic (bcc) steel and face-centered cubic (fcc) copper deformation behaviors [12]. The well-known differences persist today but with an improved understanding of the reasons for them. For example,

the role of carbon is known to produce "locking" of dislocations in grain boundary regions and to be responsible for a more-pronounced yield point behavior at smaller grain sizes [13]. The dashed curve in Fig. 3 demonstrates that the yield point can be re-established by annealing. Perhaps less well-known is the effect of increasing the applied strain rate of the test or decreasing the test temperature on moving the fcc maximum load point to a larger uniform strain [14], opposite to the more intuitive bcc result of the maximum load point moving to smaller strain values for the same changes.

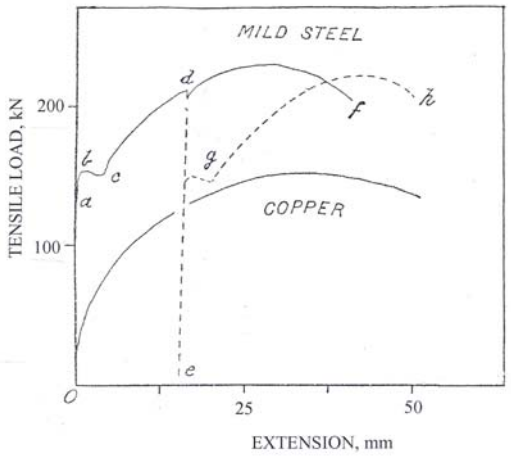

Figure 3. Unwin mild steel and copper deformation curves.

A main research effort of the 20th century was to investigate the deformation behaviors of individual fcc, bcc and hexagonal close-packed (hcp) single crystals, particularly, for the purpose of connecting the behaviors with those of polycrystalline materials. Figure 4 gives indication of bcc and fcc single crystal results. The bcc upper and lower yield point behavior is associated with carbon segregation at subgrain boundaries and the post-yield strain hardening, θ_{ath}, is essentially athermal. The fcc critical resolved shear stress, τ_{CRSS}, corresponds to "easy glide" on a primary slip system that goes over to "double slip" at τ_{II} and thereafter shows linear strain hardening at θ_{II} until reaching τ_{III} whence thermally-dependent cross-slip occurs and an approximate parabolic strain hardening ensues.

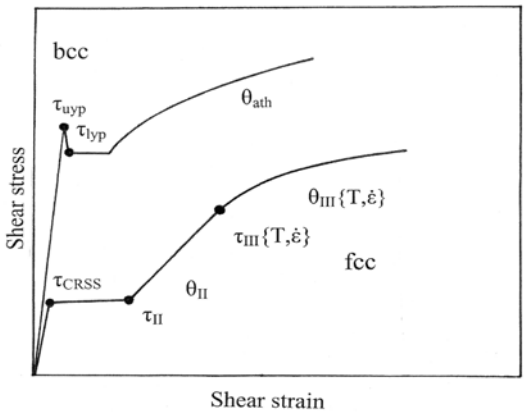

Figure 4. Schematic bcc and fcc crystal shear stress – shear strain curves.

Considerable research on deciphering the single crystal/polycrystal connection was focused on the 20th century metal, aluminum. Taylor produced a good match between the stress-strain behavior of a polycrystalline aluminum material and that of a single crystal which exhibited parabolic strain hardening from the beginning of plastic deformation [15]. A numerical factor, now well-known as the Taylor factor equal to ~3.1 was employed to multiply the crystal resolved shear stress, τ to obtain the polycrystal flow stress, σ_ε, and to divide into the resolved shear strain, γ, to obtain the polycrystal tensile strain, ε. The Taylor factor was theoretically arrived at on the assumption that five independent slip systems were necessary for plastic flow to occur within a grain of arbitrary orientation, as confirmed by a later analysis provided by Bishop and Hill [16]. Figure 5 provides a compilation of later results reported for aluminum materials whose proof stress values span single crystal, multi-crystal, and true polycrystalline results over a range of conventional grain sizes [17].

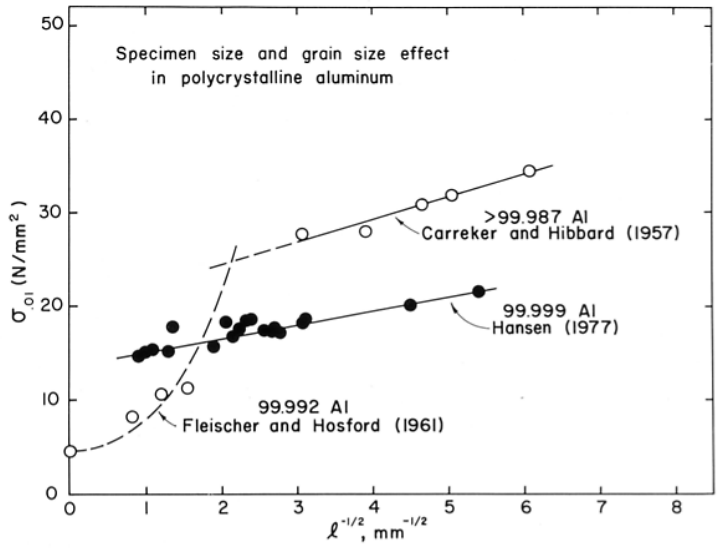

Figure 5. Initial flow stress measurements for aluminum as a function of grain size.

In Fig. 5, the topmost open circle points of Carreker and Hibbard [18] were for wire material tested over a range of temperatures and applied strain rates all following an H-P type dependence. The filled circle results were obtained for exceptionally pure material by Hansen [19] who purposely employed larger specimen sizes for the larger grain size material so as to avoid the type of specimen size effect reported by Fleischer and Hosford [20] who, in turn, made connection with the single crystal measurement shown on the ordinate stress axis.

The Fleischer and Hosford measurements have important historical connection with early results on aluminum reported by Taylor [21] and by Polanyi [22], also, for specimens with a few grains in a specimen cross-section. Taylor had argued on the basis of similar x-ray asterisms in diffraction patterns being obtained on single crystal and multi-crystal materials that the deformations were largely similar, thus presaging the later

analysis of only an orientation factor to relate the two types of deformation. Polanyi objected to Taylor's viewpoint on the basis of plastic deformation being restricted in grain boundary regions of tensile specimens as shown by (undeformed) grain boundary ridges remaining in place after tensile deformations. A modern report has been made of the opposite situation of grain boundary "valleys" observed in a compression test of aluminum 7075-T6 alloy [23].

Other aluminum results relating to the Taylor theory of single crystal/polycrystal connections were reported by Howe and Elbaum [24] and by Havner and Varadarajan [25]. The latter authors, who were concerned with taking strain-hardening into account in determining the flow stress of soft commercially pure aluminum, mentioned the need for accounting for the polycrystal grain size in reaching higher strength levels for stronger metallurgical materials. Armstrong pointed to a crystal size effect in transitioning from the testing of individual single crystals to a multi-grained material then leading to sufficient grains within a specimen cross-section to exhibit true polycrystalline behavior [26]. The issue remains a concern for small test specimens [27, 28]. It waited for Weng [29] to reconcile on a mechanics basis the Taylor and H-P descriptions even for the softest aluminum materials by building onto earlier researches focused on single crystal deformation systems operative within a polycrystal [30].

4. H-P for bcc, hcp and fcc metals

Armstrong, Codd, Douthwaite and Petch demonstrated that the H-P relation established for yielding or cleavage of mild steel applied as well for the complete stress strain behavior and that the same type H-P dependence could be applied as well to describing the yield stress or proof stress behavior of hcp and fcc metal and alloy behaviors [31].

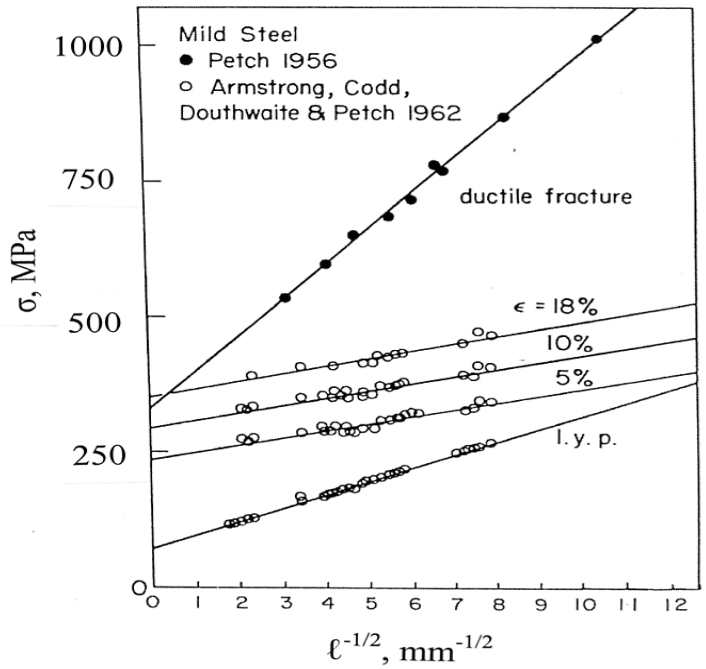

Figure 6. An H-P dependence for yield, flow and ductile fracture of mild steel.

Figure 6 provides the measurements made for mild steel. Additional H-P results were demonstrated in the same report for yield or proof stress values for aluminum, aluminum–magnesium alloy, copper, α-brass, and zinc materials. With concern for relationship to the theory of Taylor (15), a more general description of the H-P dependence was given for a material flow stress, σ_ε, at strain value, ε, as

$$\sigma_\varepsilon = m_T[\tau_{0\varepsilon} + k_{S\varepsilon}\ell^{-1/2}] \quad (1)$$

In Eq. (1), m_T is the Taylor orientation factor, $\tau_{0\varepsilon}$ is the average resolved shear stress on the operative slip systems, $k_{S\varepsilon}$ is now known as the microstructural shear stress intensity for transmission of plastic flow at grain boundaries, and ℓ is the average grain diameter [32]. Thus, the first term on the right side of Eq. (1), with $m_T\tau_{0\varepsilon} = \sigma_{0\varepsilon}$, is designated as a Taylor based component in the H-P friction stress; and $m_T k_{S\varepsilon} = k_\varepsilon$ is the microstructural stress intensity necessary to overcome the grain boundary resistance. The description of $k_{S\varepsilon}$ relates to the Griffith theory for the stress concentration associated with a shear crack, as was originally suggested in a pioneering note by Zener [33] who had proposed an analogous role for a shear crack and a slip band pile-up. An identical description of a continuum shear crack and dislocation pile-up is obtained when the pile-up is modeled in terms of a continuous distribution of infinitesimal dislocations [34, 35]. On this basis then, the H-P microstructural stress intensity description for the $k_\varepsilon\ell^{-1/2}$ term is analogous to the Griffith stress $K/(\pi c)^{1/2}$ as expressed on a fracture mechanics basis [36].

The concentrated stress on the lead dislocation in a circular double-ended pile-up was later employed to obtain a model estimation of k_ε as [32]

$$k_\varepsilon = m_T[\pi m^* G b \tau_C/2\alpha]^{1/2} \quad (2)$$

In Eq. (2), m^* is a Sachs average orientation factor for the easiest slip system for any grain orientation, G is the shear modulus, b is dislocation Burgers vector, τ_C is the local shear stress at the pile-up tip, and $\alpha = \sim 0.8$ is a measure of average dislocation line orientation. An m_T value of 2.9 applies for the bcc structure [37]. Equation (2) provides, on employment of $k_{l.y.p.} = 24$ MPa.mm$^{1/2}$ for the mild steel material result in Fig. 6, and $m_T = 2.9$, $m^* = 2.2$, $G = 80$ GPa, $b = 0.27$ nm, $\alpha = 0.84$, a value of $\tau_C = 830$ MPa = ~0.01 G, thus, giving indication of strong Cottrell locking of dislocations in grain boundary regions.

Hexagonal close-packed metals were proposed to exhibit a reasonably strong H-P dependence because of having a larger value of m_T and because of need for slip to occur at grain boundaries on prism or pyramidal slip systems in order to effect accommodation of strains [31]. Evidence for prism slip occurring in grain boundary regions of deformed magnesium polycrystals had been provided by Hauser, Landon and Dorn [38]. The same authors had also provided H-P $\sigma_{0\varepsilon}$ and k_ε measurements as a function of temperature [39]. Armstrong [40] correlated the reported temperature-dependent H-P parameters with available measurements of τ_{CRSS} values for (lower) basal and (higher) prism slip systems in accordance with the predictions of Eqs. (1) and (2). Figure 7 shows a modern

compilation of H-P results for magnesium and for several AZ31 magnesium alloy materials. The dashed inset contains the conventional grain size results obtained at ambient temperature in the pioneering study by Hauser, Landon and Dorn of proof stress values for reasonably pure material absent any crystallographic texture [38]. Caceres and Blake reported complementary yield stress results also with essentially equivalent yield stresses both in tension and compression for texture-free material [41]. They obtained a value of k_ε = ~10.8 MPa.mm$^{1/2}$ as compared with k_ε = ~8.8 MPa.mm$^{1/2}$ from Hauser *et al*. With $m_T = m^*$ = ~6.5, G = 17.5 GPa, b = 0.32 nm, τ_C = 40 MPa, and α = 0.84, a value of k_ε = 10.6 MPa.mm$^{1/2}$ is computed from Eq. (2).

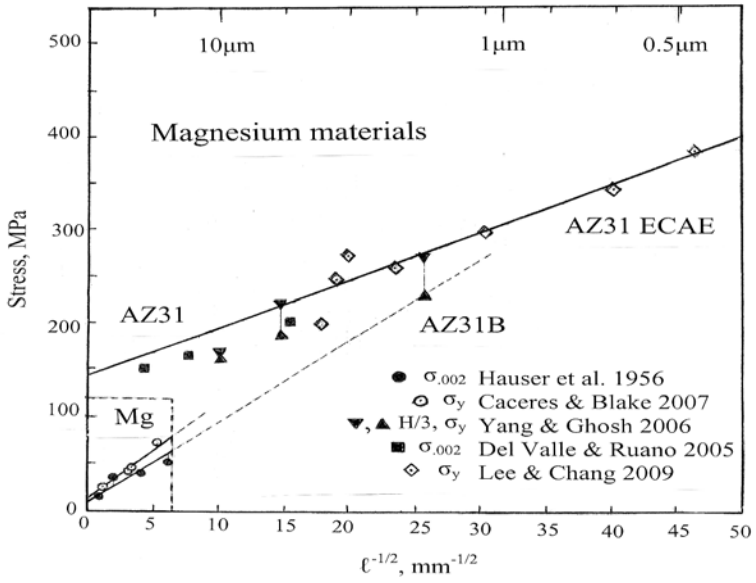

Figure 7. An H-P dependence for magnesium and AZ31 alloy materials.

The mostly smaller grain size AZ31 magnesium alloy materials shown in Fig. 7 were produced by relatively heavy deformations associated with the equal channel angular extrusion (ECAE) and annealing technique [42-44]. The technique relates to specification also as equal channel angular pressing (ECAP). Yuan , Panigrahi, Su and Mishra have given a tabulation of H-P results for AZ31 materials prepared by these techniques [45]. The H-P results included grain sizes smaller than ~10 micrometers and included microstructural stress intensity values in the range $5.1 \leq k_\varepsilon \leq 11.0$ MPa.mm$^{1/2}$. The k_ε values are in line with those shown for the AZ31 materials in Fig. 7 and are explained relative to the magnesium results in terms of influence of texture on lowering of m_T and m^* values plus an increase of prism slip in $\sigma_{0\varepsilon}$. Pioneering results on the influence of texture in lowering k_ε for variously processed magnesium material had been reported by Wilson and Chapman [46].

Weng entered an H-P dependence into the analysis of polycrystalline deformation as previously formulated on the basis of continuum plasticity descriptions associated with the pioneering researches of Taylor, Hill, Prager and others [29]. A micromechanics connection was made by employing an expanded version of the square-bracketed shear stress factor in Eq. (1) in summing of individual grain deformations to describe the grain

size dependent stress – strain results. Under presumed multi-slip conditions, the shear stress dependence on strain was expressed for the *i*th slip system within a single grain as

$$\tau_\varepsilon = (\tau_y + k_y \ell^{-1/2}) + (h + a\ell^{-1/2}) \sum_j [\alpha' + (1-\alpha') \cos\theta^{i,j} \cos\varphi^{i,j}] (\gamma^p)^n \quad (3)$$

In addition to an initial H-P determined yield stress contained within the first parentheses on the right side of Eq. (3), a second term for H-P type strain hardening, with coefficients of *h* and *a*, was included to multiply, with $\alpha' = 0$, Prager type kinematic hardening among *i*th and *j*th slip systems related through (θ, φ) for an assumed power law hardening with exponent *n* of the plastic shear strain, γ^p. Under condition of $\alpha' = 1$, the form of Eq. (3) would be equivalent to Taylor's theory of isotropic strain hardening, except for the included H-P dependence. In turn, a formalism was employed to show how Eq, (3) would add on to the Taylor type consideration for summing over the needed slip systems in order to specify the local stress operative within a single grain.

Weng applied his analysis to detailed H-P measurements reported by Hansen and Ralph for the tensile plastic stress – strain behavior of copper [47]. A reasonably constant grain size dependence had been obtained experimentally with $k_\varepsilon = \sim 5.0$ MPa.mm$^{1/2}$. The major strain hardening behavior was in $\sigma_{0\varepsilon}$. Note that the behavior is similar to that shown in Fig. 1 for mild steel past the initial yield point behavior. Weng's model description, with α' necessarily assumed to be 1.0 for Taylor isotropic hardening led to a very good match with the experimental results. For example, employing Taylor's $m_T = 3.1$ and Weng's computed value of $m_T k = m_T k_{S\varepsilon} = \sim 3.74$ MPa.mm$^{1/2}$ at $\varepsilon = 0.05$ plus addition of a computed value of the grain size dependent increment of strain hardening term, $\Delta k_{S\varepsilon} = h = \sim 0.68$ MPa.mm$^{1/2}$, a value of $k_\varepsilon = \sim 4.42$ MPa.mm$^{1/2}$ is estimated.

5. Conventional to nano-scale H-P results

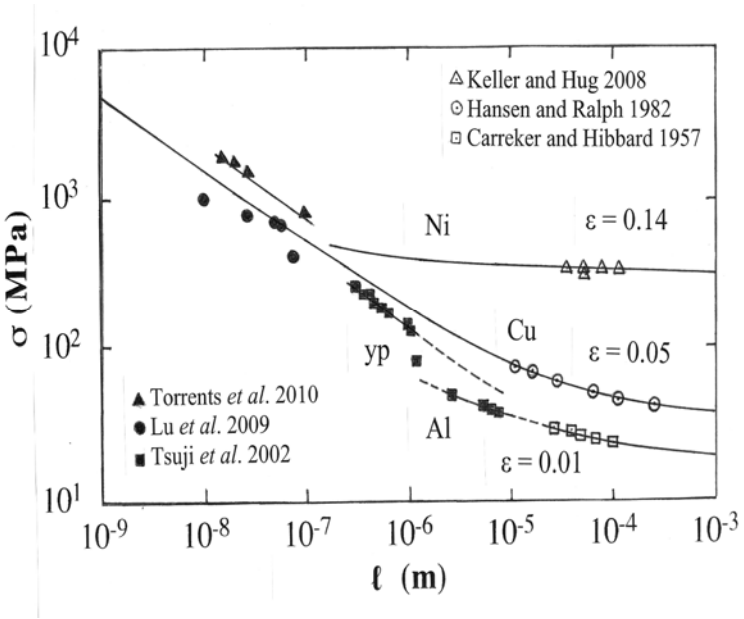

Figure 8. Conventional and ultra-fine grain size H-P dependencies for Al, Cu and Ni.

Figure 8 provides another basis on which to compare the contributions of strain hardening, in $\Delta\sigma_{0\varepsilon}$, and of grain size refinement, in $k_\varepsilon \ell^{-1/2}$, on determining the flow stress of fcc metals. The same Hansen and Ralph results employed by Weng are shown at ε = 0.05 for the open circle points in the figure. The previously referenced Carreker and Hibbard results [19] shown for aluminum in Fig. 5 are plotted as the open square points. On such log/log basis, Eq. (1) goes over to a constant value of $\sigma_{0\varepsilon}$ at large grain diameter and moves asymptotically to a linear dependence of slope (-1/2) at smaller grain sizes. The topmost open triangle points for nickel material at conventional grain sizes are for the indicated ε = 0.14 measurements reported by Keller and Hug [48]. These results involved a significant increase in $\sigma_{0\varepsilon}$ from 14.23 MPa at ε = 0.002 to 311 MPa at the indicated strain in Fig. 8 but showed a reduction from $k_{.002}$ = ~5.17 MPa.mm$^{1/2}$ to $k_{.14}$ = ~2.15 MPa.mm$^{1/2}$. The atypical behavior of a reduction in k_ε on uniform straining might possibly be explained by the development of an exaggerated grain texture during straining. A weak texture had been reported for the initial material and measurements (not shown here) were presented for an unusually large value of $k_{.14}$ for larger grain size material. It should be noted that the initial proof stress measurements of k_ε for the copper and nickel materials have very nearly the same value.

There is greater interest in Fig. 8 in connection of the conventional grain size H-P behaviors for all three metals with the results shown at the smaller ultrafine grain sizes. The closed triangle measurements shown for nickel at the smallest grain sizes were obtained from transformation of diamond pyramid hardness measurements, *H*, on the well-established basis of $\sigma_\varepsilon = H/3$. The closed circle results were compiled by L. Lu, Chen, Huang and K. Lu from a number of reported measurements by different investigators [49]. Lu et al. were concerned with comparing those results with an H-P description of nano-twinned material, to be described and for which the twin spacing was taken equal to the effective grain diameter. Armstrong *et al.* had discussed the issue of annealing or deformation twin boundaries being involved in strengthening α-brass or zinc materials [31]. And, lastly in Fig. 8, the somewhat offset displacement of the aluminum results of Carreker and Hibbard compared to those of Tsuji, Ito, Saito and Minamino [50] relate to the appearance of a significant yield point behavior as the grain size was refined. A lower commercial purity of 99.3 % purity applied for the Tsuji *et al.* material. The importance of purity for aluminum was already indicated in Fig. 5 for the results of Carreker and Hibbard [18] as compared with those of Hansen [19]. In Fig. 8, the value of k_y = ~ 3.5 MPa.mm$^{1/2}$ obtained at larger grain size by Tsuji *et al*. was increased to ~4.8 MPa.mm$^{1/2}$ at smaller grain sizes. The behavior relates to the higher $k_{l.y.p}$ for the yield point enhancement of demonstrated for steel in Fig. 6.

Armstrong and Smith had considered, in relating conventional and ultrafine grain size copper results of the type shown in Fig. 8, what might be the smallest number of dislocations that could be fitted into a smallest grain size material [51]. Such consideration had been involved previously in accounting for the ultra-high strength of patented steel wire material [52]. Figure 9 shows evaluation of the consideration for extension into the nano-scale regime of the Hansen and Ralph measurements. For a

circular dislocation pile-up, the relation between number of dislocation loops, n, the grain size, ℓ, and k_ε is

$$n = 2\alpha k_\varepsilon \ell^{1/2}/\pi m_T G b \quad (4)$$

The condition for $n = 1.0$ is shown in Fig. 8 on a σ vs. ℓ basis at the transition of the H-P extrapolation into a dashed line. Also, the relationship for expansion of a single dislocation loop against the grain boundary resistance is established by addition of τ_C to the single loop equation of Li and Liu [53] as

$$\sigma = m_T[\tau_0 + (3Gb/4\pi\ell)\{(5/6)(\mathbf{ln}[4\ell/b] - 1) - 1/16\} + \tau_C] \quad (5)$$

The constants τ_0 and τ_C are obtained from the Hansen and Ralph H-P results, employing in the latter case, Eq. (2). Equation (5) is shown in Fig. 9 as the lower dashed curve beginning from large grain size that transitions to extension of the H-P dependence at the $n = 1.0$ condition; the upper dashed line is a limiting theoretical stress estimation. The offset jump in stress is a result of the analytic approximations made in the continuum description. Thus, the model description leads to the observation that the limiting pile-up transition to a single dislocation loop expanding against the grain boundary resistance should produce an increase in stress for the extended H-P relation.

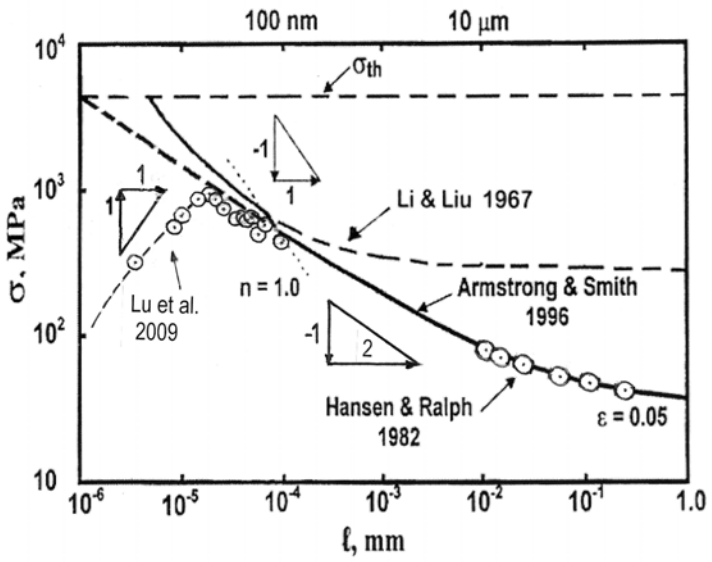

Figure 9. H-P transition to a single loop expanding against the grain boundary resistance.

The smaller abscissa open circle points plotted in Fig. 9 for nano-twinned copper results, coincidentally positioned at the break in the H-P dependence, were reported by Lu *et al*. [49] for pulse-deposited material having twin spacings, λ, taken as the effective grain diameter. At the smallest twin spacings however, a reversed H-P dependence was observed and credited to effective grain boundary weakening. The behavior is of interest in consideration of complementary strain rate sensitivity measurements that are to be described for both types of behavior.

6. The H-P connected strain rate sensitivity

The activation volume parameter, v^*, is defined by differentiation of the logarithm of the plastic shear strain rate, ($d\gamma/dt$) with respect to the thermal component of stress, τ_{Th}, in the relationship involving multiplication by Boltzmann's constant, k_B, and temperature, T, as

$$v^* = k_B T[\partial\{\mathbf{ln}(d\gamma/dt)\}/\partial\tau_{Th}]_T \quad (6)$$

The v^* parameter, interpreted as the product of b and an activation area, A^*, for thermally overcoming of a local obstacle, provides a theoretical model basis relating to Fig. 4 for evaluating the various dislocation mechanisms involved in determining either the thermal dependence in the yield stress of bcc metals or in the strain hardening property of fcc metals [54]. For example, an examination of the dislocation pile-up based interpretation of the H-P parameters leads to potential thermal activation both in the frictional shear stress, $\tau_{0\varepsilon}$, and in the τ_C factor in $k_{S\varepsilon}$. Whereas the value of τ_C specified with respect to Eq. 2 for $k_{l.y.p}$ of α-iron is too high for thermal activation, the situation is different for the lower k_ε values of certain hcp metals and for pure fcc metals [55].

Prasad and Armstrong reported an H-P type dependence for the reciprocal value of v^* obtained by differentiation of the H-P relation, including τ_C in k_ε, as [56]

$$v^{*-1} = v_0^{*-1} + (k_\varepsilon/2m_T\tau_C v_C^*)\ell^{-1/2} \quad (7)$$

In Eq. (7), v_0^* is the activation volume determined by the strain rate dependence in $\sigma_{0\varepsilon}$ and v_C^* is the activation volume determined from the thermal shear stress component of τ_C in k_ε. Indication that there should be both grain volume and grain boundary contributions to v^* was provided in the separate thermal stress associations established for magnesium of basal slip being responsible for $\sigma_{0\varepsilon}$ and prism slip being responsible for k_ε; see the discussion centered on magnesium in Section 4 and reference [40]. On the basis of Armstrong having shown previously that the product of $\tau_{Th}v^*$ was constant for various thermally-dependent dislocation mechanisms in hcp, fcc, and bcc single crystals [57], Prasad and Armstrong proposed that Eq. (7) should follow its own H-P type dependence and provided evidence for the validity of the relationship in results reported for polycrystalline cadmium material. Later similar results were reported for polycrystalline zinc material [58] and for additional detailed measurements reported for other cadmium measurements [59]. The H-P type dependence of Eq. (7) has been demonstrated for compiled v^* measurements reported for magnesium [60].

In a review of extensive measurements reported for the plastic deformation of aluminum polycrystal measurements, Armstrong proposed that a need for cross-slip to occur for transmission of plastic flow at grain boundaries provided a ready explanation of the low value of k_ε [17]. Additional evidence that cross-slip played the same role for copper was presented in a demonstration of k_ε^2 and τ_{III} following parallel temperature and strain rate dependencies [55], as had been demonstrated for the parallel temperature dependencies for H-P parameters with basal and prism slip in magnesium single crystals

and polycrystals. More recently, Armstrong has pointed to a cross-slip explanation of copper and nickel materials having nearly the same values of k_ε because, whereas the shear modulus of nickel is about two times larger than the shear modulus of copper, the nickel cross-slip stress, τ_{III}, is approximately one-half of that of nickel; see the tabulation of cross-slip measurements reported by Bell (61).

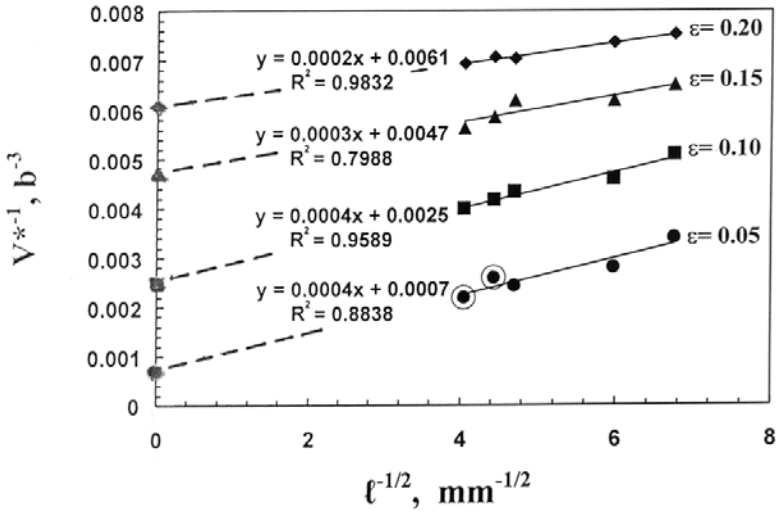

Figure 10. H-P dependence for v^{*-1} measurements reported for nickel.

Narutani and Takamura provided important v^* measurements for polycrystalline nickel materials over a range of conventional grain sizes [62]. The measurements had been converted to a dislocation density interpretation on the basis of dislocation intersections being the controlling mechanism for the thermally-dependent strain hardening. And a greater dislocation density was computed on the basis of the v^* measurements when compared with independent density measurements determined by calibrated electrical resistivity measurements. Narutani and Takamura explained the disparity in terms of the v^* result being representative of a greater local dislocation density. Subsequently, the reported v^* measurements were shown by Rodriguez [63] to follow Eq. (7) that provided in Fig. 10 a separation of larger v_0^* values for dislocation intersections within the grain volumes and smaller v_C^* values associated with τ_C for cross-slip at the grain boundaries.

7. Nano-scale nickel and copper v^* measurements

Armstrong and Rodriguez [64] employed Eq. (7) to show connection of conventional and nano-scale measurements of v^* as shown in the compilation of combined nickel and copper results plotted in Fig. 11. The filled circle points are those from Fig. 10 at ε = 0.05. The top solid curve is the H-P relation obtained for the results measured at 195 K and the lower curve is the estimated H-P type result for 300 K. The open square, open diamond, and closed diamond points were reported by Asaro and Suresh for a combination of nickel and copper measurements [65]. The two cross points were added by Weng [66] from measurements reported by Schwaiger, Moser, Dao, Chollacoop and Suresh [67]. The open circle points were obtained for the nano-twinned material of Lu *et*

al. [49] who produced the H-P strengthening and weakening dependencies shown in Fig. 9. Of particular interest now are the higher v^* values associated with the effective grain size weakening results and are indicated in the figure (with $k = k_B$) to have a different relationship for v^{*-1}.

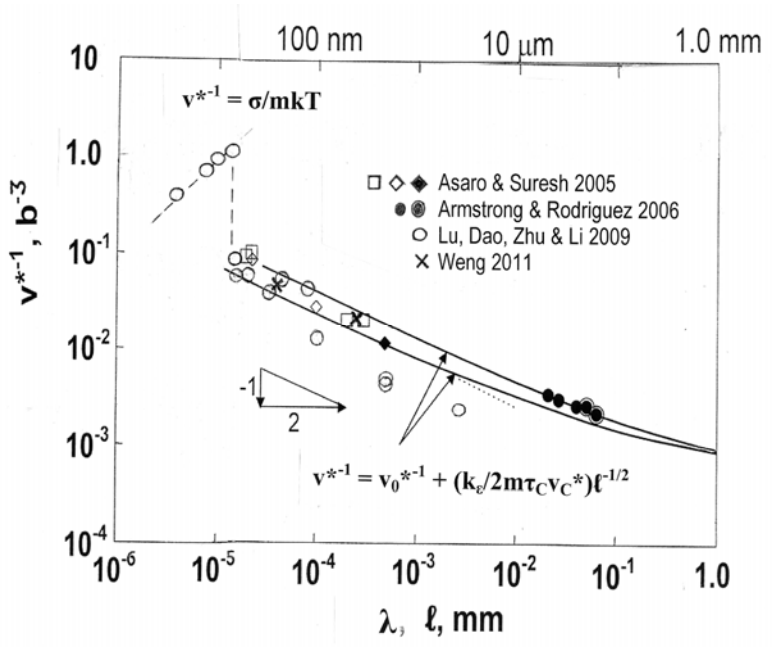

Figure 11. Nickel and copper v^{*-1} measurements at nano-twin and nano-grain sizes.

The several constitutive equations reported thus far in the literature to explain H-P type grain size weakening have their roots in analyses of higher temperature creep deformations, for example, as discussed by Armstrong, Conrad and Nabarro [68]. A usual type equation for the tensile or compressive strain rate, ($d\varepsilon/dt$), has been given by Langdon [69] as

$$(d\varepsilon/dt) = (AD_iGb/k_BT)(b/\ell)^p(\sigma/G)^q \qquad (8)$$

In Eq. (8), D_i is a diffusion coefficient for mass transport within the grain volumes or at grain boundaries and A, p and q are experimental constants; for example, $p = 2.0$ and $q = 1.0$ for Nabarro-Herring creep. Armstrong [60] had taken p = q = 1.0 in Eq. (8), to obtain by differentiation a reversed trend for v^* in accordance with the relationship

$$v^* = \sigma/m_T k_B T \qquad (9)$$

Thus in the grain size weakening regime, a reversed dependence of v^* on grain size should be expected in accordance with the reversed H-P dependence of σ. The same type v^* dependence shown in the figure was described previously for reversed nano-scale strength measurements reported by Conrad and Narayan [70]. And the smaller than atomic dimension values of v^* that were obtained were taken to be reflective of thermal activation associated with grain boundary diffusion or shearing mechanisms at the grain

boundaries. The reversed measurements shown in Fig. 11 may possibly have a similar explanation for the deformation behavior at the copper twin boundaries or perhaps be associated with partial dislocation activity.

8. Grain boundary disorder in nano-scale materials?

Figure 12 returns to the relationship of conventional and nano-scale grain size results but obtained in this case for the strength of iron and steel materials. The compiled measurements cover a range of material types and conditions: the open square points are for drawn eutectic steel wires [71]; and, the open circle points are for ball-milled α-iron material [72]. The open diamond points are transformed from highest hardness measurements reported for α-iron material [73]; and, the open triangle measurements are for interstitial free (IF) α-iron [74]. The solid line, and including the other filled circle, triangle and square points associated with it, was reported earlier [75] in an investigation based on the lower yield point H-P dependence shown in Fig. 6. The short dashed line segments through the open square points and open circle ones were suggested to be representative of a reduced k_ε value associated with disordered grain boundary structures at the smallest material grain sizes [76]. The suggestion is supported by the indication at larger grain sizes of a higher value of $\sigma_{0\varepsilon}$ for the ball-milled (open circle) material. For comparison with the shifted H-P lines, the longer dashed H-P dependence drawn for the open triangle points corresponds to reduced values of $\sigma_{0\varepsilon}$ = ~43 MPa and k_ε = ~11 MPA.mm$^{1/2}$ for the IF material.

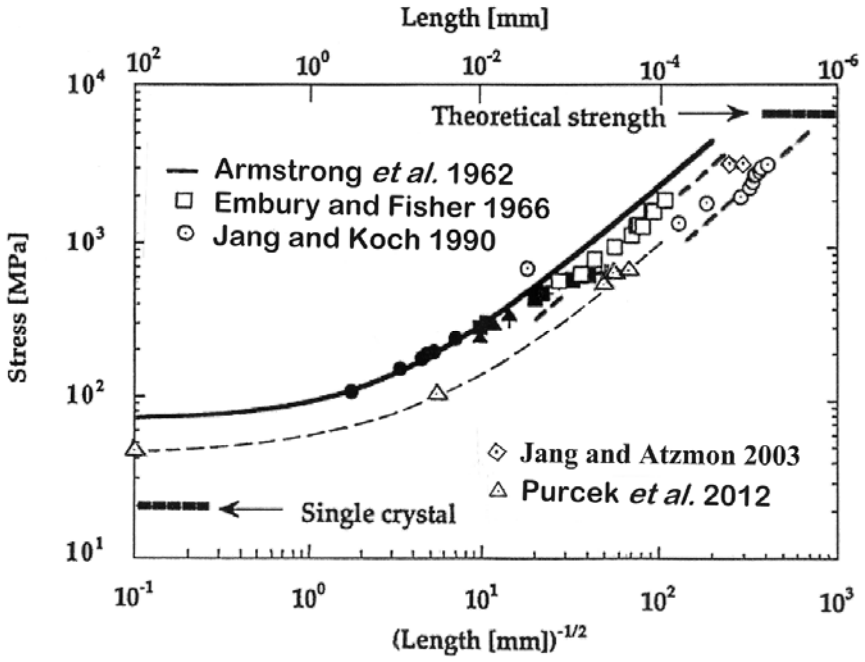

Figure 12. H-P results for mild steel and interstitial free α-iron.

9. Discussion

Weng [66] and Armstrong [60] contributed complementary articles on model composite and dislocation mechanics aspects, respectively, of nanopolycrystalline metal

strength and strain rate sensitivity properties. It is interesting to track the development of other composite model descriptions based on a continuum mechanics viewpoint. For example, Carsley, Ning, Milligan, Hackney and Aifantis presented a composite mixtures based model for nano-scale material consisting of an intragranular crystalline material encompassed by an amorphous grain boundary phase [77]. The preceding discussion centered on Fig. 12 of disordered grain boundaries possibly being produced in at least some nanocrystalline materials was referenced to the early 20th century model description of Rosenhain and Ewen for an amorphous grain boundary structure [76]. Paired grain and grain boundary regions were described in an early report by Jiang and Weng [78]. In addition to the earlier referenced Taylor-based assessments of crystallographic slipping within the grains [29], such slipping was taken also to be limited by an amorphous grain boundary region. As before, the model was employed to describe an H-P dependence for copper material but, below a critical nano-scale grain size, a transition to weakening occurred under grain boundary control. The nanocrystalline model consideration was further developed in the secant viscosity composite model investigated by Li and Weng [79] who added important consideration thereby of the material strain rate sensitivity. The strain rate sensitivity results reported for nickel by Schwaiger et al. [67] were accounted for in the model predictions; see also Fig. 11. Within the same secant viscosity model, Barai and Weng attributed the deformation properties to three structural mechanisms: (1) dislocation flow within the grain interior; (2) grain boundary deformations via uncorrelated atomic displacements within grain boundary zones; and, (3) grain boundary sliding at the interfaces of the zones. Analysis of strain rate sensitivity measurements made on copper in the grain size weakening regime were stated to agree with the trend of predicted results reported by Rodriguez and Armstrong on zinc [80] and similarly shown here for copper in Fig. 11. Most recently, Li and Weng have presented a review of the model with special regard for v^* predictions [81].

The present description relates to other considerations of polycrystal deformations and the consequent material strength properties. Anand has pointed to the anisotropic plastic response, particularly at large deformations, of a polycrystalline fcc material being solely explained on the basis of the crystallographic texture developed by reorientation of the lattice structure of the grains [82]. There is a considerable history on the topic relating to Taylor's analysis for fcc metals. Kim and Oh presented a two-dimensional finite model analysis of joined grain deformations incorporating couple stresses to account for the influence of grain size [83]. Armstrong and Zerilli have discussed the influence of grain reorientations on k_ε and the development of plastic instability and shear banding behavior that is of greater concern for bcc and hcp metals [84]. For magnesium, there is a considerable influence of reduction in grain size on increase of the material ductility [85] that has been correlated with the H-P parameters [86].

The issue of plastic instability bears on the early observation by Petch [87] of an H-P dependence for the ductile fracture stress as shown in Fig. 6. The flow stress at $\varepsilon = 0.18$ in Fig. 6, was essentially equal to the maximum load stress for uniform deformation and therefore the subsequent increase in the H-P stress was determined by the strain hardening that occurred during the local necking strain. A same H-P dependence was demonstrated to apply for the tensile ductile fracture stress of aluminum at low

temperature by Chin, Hosford and Backofen [88]. The topic has been investigated more recently in an important article by Massart and Pardoen describing an analysis of results reported on pure iron and IF iron materials [89]. These authors employ a highest experimental value of σ_y = ~2.68 GPa for material with a grain size of 80 nm. The result agrees very well with the H-P evaluation in Fig. 6 employing $k_{l.y.p}$ = 24 MPa.mm$^{1/2}$. An H-P dependence fits the full range of experimental measurements that extended to a grain size of 10 micrometers. A loss of ductility occurring after reduction to a grain size of ~1.0 micrometer was attributed to the limited strain hardening capacity of the material. Liu, Armstrong and Gurland had attributed such behavior found for a number of steel materials at that same grain size to their limited strain hardening behavior [90]. And, relating to the same type of observation, Lu et al. attribute an enhanced ductility for their nano-twinned copper material to the generation of dislocations at the coherent twin boundary interfaces [49]. Recent results reported for drawn pearlitic steel wire material have also pointed to the importance of dislocation generations in the ultrafine material structure [91]. The topic is further considered along with additional aspects of a broader range of H-P connected material properties in another report [92].

10. Summary

The present article has been developed to honor the accomplishments of Professor Weng, current Prager Medallist, who with students and colleagues, has made leading mechanics contributions to our understanding of the influence of crystal lattice and grain size on the strength properties of polycrystalline metals. In the present report, after an initial description of historical aspects of the topic beginning in the 18th century and relating to the characterization of polycrystal microstructures that took hold in the late 19th century due to the pioneering researches of Sorby [93], focus was put on researches in the 20th century dealing with polycrystal grain morphologies, single crystal plasticity, and its relation to polycrystal deformations. George Weng introduced the Hall-Petch description into a proper micromechanical model of polycrystalline deformations, consistent with concurrent dislocation mechanics theory. The work has been shown to be extended into this 21st century with emphasis placed on both the strength and strain rate sensitivity properties of nanopolycrystalline materials.

Acknowledgements

Appreciation is expressed to Jackie Li for the invitation to participate in the Prager Medal Symposium honoring George Weng and, especially, thanks are expressed to George for his friendship over the years.

References

1. R.W. Armstrong, “Hall-Petch analysis from a combined mechanics and materials viewpoint”, Mechanical and Aerospace Engineering Colloquium Series, 4/17/13, Rutgers, The State University of New Jersey, Piscataway, http://www.cecd.umd.edu

2. R.A.F. de Reaumur, “On methods of recognizing defects and good quality in steel and on several ways of comparing different grades of steel”, in L’Art de Convertir le Fer Forge en Acier (Paris, 1722) pp. 63-106; transl. A.G. Sisco (Chicago, 1956) pp. 176-204.

3. P.C. Grignon, “On the metamorphoses of iron”, in Memoires de Physique sur l’Art de Fabriquer de Fer” (Paris. 1775) pp. 56-90, transl. P. Boucher and C.S. Smith, in Sources for the History of the Science of Steel 1532-1786 (The Society for the History of Technology and the M.I.T. Press, Cambridge, MA, 1968) pp. 125-164.

4. C.S. Smith and J.G. Burke, Atoms, Blacksmiths and Crystals; Practical and Theoretical Views of the Structure of Matter in the Seventeenth and Eighteenth Centuries (William Andrews Clark Memorial Library, Univ. California, Los Angeles, 1967).

5. C.S. Smith, “Introduction to grains, phases, and interfaces – an interpretation of microstructure”, Trans. TMS-AIME **175**, 15-51 (1948).

6. C.S. Smith, “Further notes on the shape of metal grains: Space –filling polyhedra with unlimited sharing of corners and faces”, Acta Metall. **1**, 295-300 (1953).

7. F.N. Rhines, K.R. Craig and R.T. DeHoff, “Mechanism of steady-state grain growth in aluminum”, Metall. Trans. **5**, 413-425 (1974).

8. R.W. Armstrong, “Strengthening mechanisms and brittleness in metals’, J. Ocean Engng. **1**, 239-256 (1969).

9. K. Jagannadham and R.W. Armstrong, “Evidence for dislocation pile-ups at grain boundaries from slip band step height observations”, Scr. Metall. **21**, 1459-1462 (1987).

10. J.P. Gudas, G.R. Irwin, R.W. Armstrong and X.J. Zhang, “A model for transition fracture of structural steels from observations of isolated cleavage regions”, ed. by J.G. Blauel and K.-H. Schwalbe, Defect Assesssment in Components – Fundamentals and Applications, ESIS/EGF9 (Mech. Eng. Publ. Ltd., London, 1991) pp. 549-568.

11. R.W. Armstrong, “Dislocation mechanics description of polycrystal plastic flow and fracturing behaviors”, Mechanics and Materials: Fundamentals and linkages, ed. by M.A. Meyers, R.W. Armstrong and H. Kirchner (John wiley and Sons, Inc., N.Y., 1999) Ch. 10, pp. 363-398.

12. W.C. Unwin, “On the yield point of iron and steel and the effect of repeated straining and annealing”, Proc. Roy. Soc. Lond. **57**, 178-187 (1894).

13. N. J. Petch, “Theory of the yield point and strain-ageing in steel”, Advances in Physical Metallurgy; Sir Alan Cottrell’s 70th Birthday Meeting, ed. by J.A. Charles and G.C. Smith (Inst. Met., London, 1990) pp. 11-25.

14. R.W. Armstrong and F.J. Zerilli, "Dislocation mechanics based viscoplasticity description of fcc, bcc and hcp metal deformation and fracturing behavior", Proc. ASME Mater. Div. (ASME, N.Y., 1995) MD-69-1, pp. 417-428.

15. G.I. Taylor, "The mechanism of plastic deformation of crystals; Part I.-Theoretical", Proc. Roy. Soc. Lond., **145**, 362-387 (1934).

16. J.F.W. Bishop and R. Hill, "A theoretical derivation of the plastic properties of a polycrystalline face-centered metal", Philos. Mag., **42**, 1298-1307 (1951).

17. R.W. Armstrong, "Dislocation queueing analysis for the plastic deformation of aluminum polycrystals", Physics of Materials; A Festschrift for Dr. Walter Boas on the occasion of his 75th Birthday", ed. by D.W. Borland, L.M.. Clarebrough and A.J.W. Moore (CSIRO and Univ. Melbourne Press, Australia, 1979) pp. 1-11.

18. R.P. Carreker, Jr. and W.R. Hibbard, Jr., "Tensile deformation of aluminum as a function of temperature, strain rate and grain size", Trans. TMS-AIME **209**, 1157-1163 (1957).

19. N. Hansen, "Effect of grain size and strain on the tensile flow stress of aluminum at room temperature", Acta Metall. **25**, 863-869 (1977).

20. R.L. Fleischer and W.F. Hosford, Jr., "Easy glide and grain boundary effects in polycrystalline aluminum", Trans. TMS-AIME **221**, 244-247 (1961).

21. G.I. Taylor, "Resistance to shear in metal crystals", Trans. Faraday Soc., **XXIV**, 121-126 (1928).

22. M. Polanyi, "Deformation, rupture and hardening of crystals", Trans. Faraday Soc., **XXIV**, 72-83, 172 (1928).

23. Tech Notes: "Orange Peel", Adv. Mater. Proc., **163**, [7], p. 50 (2005).

24. S. Howe and C. Elbaum, The relation between the plastic deformation of aluminum single crystals and polycrystals, Philos. Mag. **6**, 37-48 (1961).

25. K.S. Havner and R. Varadarajan, "A quantitative study of a crystalline aggregate model", Int. J. Sol. Struct., **9**, 379ff (1973); *Ibid.* **13**, 395 (1977).

26. R.W. Armstrong, "On size effects in polycrystal plasticity", J. Mech. Phys. Sol. **9**, 196-199 (1961).

27. C. Keller and E. Hug, "Hall-Petch behavior of Ni polycrystals with a few grains per thickness", Mater. Letts., **62**, 1718-1720 (2008).

28. H. Justinger and G. Hirt, “Estimation of grain size and grain orientation influence in microforming processes by Taylor factor considerations”, J. Mater. Proc. Tech. **209**, 2111-2121 (2009).

29. G.J. Weng, “A micromechanical theory of grain-size dependence in metal plasticity”, J. Mech. Phys. Sol., **31**, 195-203 (1983).

30. G.J. Weng and A. Phillips, “The stress fields of continuous distributions of dislocations and of their movement in a polycrystalline aggregate”, Int. J. Sol. Struct., **14**, 535-544 (1978).

31. R.W. Armstrong, I. Codd, R.M. Douthwaite and N.J. Petch, “The plastic deformation of polycrystalline aggregates”, Philos. Mag.,**7**, 45-58 (1962).

32. R.W. Armstrong, “The yield and flow stress dependence on polycrystal grain size”, Yield, Flow and Fracture of Polycrystals, ed. by T.N. Baker (Appl. Sci. Publ., London, 1983) Ch. 1, pp. 1-31.

33. C. Zener, “A theoretical criterion for the initiation of slip bands”, Phys. Rev., **69**, 128-129 (1946).

34. L.M. Keer, “A note on shear and combined loading for a penny-shaped crack”, J. Mech. Phys. Sol., **14**, 1-8 (1966).

35. H.W. Liu and Q. Gao, “The equivalence between dislocation pile-ups and cracks”, Theor. Appl. Fract. Mech., **12**, 195-204 (1990).

36. R.W. Armstrong, “Dislocation viscoplasticity aspects of material fracturing”, Eng. Fract. Mech., **77**, 1348-1359 (2010).

37. J.W. Hutchinson, “Plastic deformation of bcc polycrystals”, J. Mech. Phys. Sol., **12**, 25- (1964).

38. F.E. Hauser, P.R. Landon and J.E. Dorn, Trans. Amer. Soc. Met., **48**, 986- (1956).

39. F.E. Hauser, P.R. Landon and J.E. Dorn, “Fracture of magnesium alloys at low temperature”, Trans. TMS-AIME, **206**, 589-593 (1956).

40. R.W. Armstrong, “Theory for the tensile ductile-brittle behavior of polycrystalline hcp materials; with application to beryllium”, Acta Metall. **16**, 347-356 (1968).

41. C.H. Caceres and A. Blake, “On the strain hardening behavior of magnesium at room temperature”, Mater. Sci. Eng. A, **462**, 193-196 (2007).

42. Q. Yang and A.K. Ghosh, “Deformation behavior of ultrafine-grain (UFG) AZ31B Mg alloy at room temperature”, Acta Mater., **54**, 5159-5170 (2006).

43. J.A. Del Valle and O.A. Ruano, “Influence of grain size on the strain rate sensitivity in an Mg-Al-Zn alloy at moderate temperatures”, Scr. Mater., **55**, 775-778 (2006).

44. W.-T. Lee (and C.P. Chang), Ph.D. Thesis (2011) Nat. Sun Yat-Sen University, TW.

45. W. Yuan, S.K. Panigrahi, J.-Q. Su and R.S. Mishra, “Influence of grain size and texture on Hall-Petch relationship for a magnesium alloy”, Scr. Mater., **65**, 994-997 (2011).

46. D.V. Wilson and J.A. Chapman, “Effects of preferred orientation on the grain size dependence of yield strength in metals”, Philos. Mag., **8**, 1543-1551 (1963).

47. N. Hansen and B. Ralph, “The strain and grain size dependence of the flow stress of copper”, Acta Metall., **30**, 411-417 (1982).

48. C. Keller and E. Hug. “Hall-Petch behavior of Ni polycrystals with a few grains per thickness”, Mater. Letts., **62**, 1718-1720 (2008).

49. L. Lu, X. Chen, X. Huang and K. Lu, “Revealing the maximum strength in nanotwinned copper”, Science, **323**, 607-610 (2009).

50. N. Tsuji, Y. Ito, Y. Saito and Y. Minamino, “Strength and ductility of ultrafine grained aluminum and iron produced by ARB and annealing”, Scr. Mater., **47**, 893-899 (2002).

51. R.W. Armstrong and T.R. Smith, “Dislocation pile-up predictions for the strength properties of ultrafine grain size fcc metals”, Processing and Properties of Nanocrystalline Materials, ed. by C. Suryanarayana, J. Singh and F.H. Froes (TMS-AIME, Warrendale, PA, 1996) pp. 345-354.

52. R.W. Armstrong, Y.T. Chou, R.M. Fisher and N. Louat, “The limiting grain size dependence of the strength of a polycrystalline aggregate”, Philos. Mag., **14,** 943-951 (1966).

53. J.C. M. Li and G.C.T. Liu, “Circular dislocation pile-ups: I. Strength of ultrafine polycrystalline aggregates”, Philos. Mag., **15**, 1059-1063 (1967).

54. R.W. Armstrong and S.M. Walley, “High strain rate properties of metals and alloys”, Int. Mater. Rev., **53**, 105-128 (2008).

55. R.W. Armstrong, “Strength and ductility of metals”, Trans. Ind. Inst. Met., **50**, 521-531 (1997).

56. Y.V.R. K. Prasad and R.W. Armstrong, “Polycrystal versus single crystal strain rate sensitivity of cadmium”, Philos. Mag., **29**, 14210-1425 (1974).

57. R.W. Armstrong, “Thermal activation – strain rate analysis (TASRA) for polycrystalline metals”, (Ind.) J. Sci. Indust. Res., **32**, 591-598 (1973).

58. Y.V.R.K. Prasad, N.M. Madhava and R.W. Armstrong, “Strengthening of hcp metals due to the presence of grain boundaries”, Grain Boundaries in Engineering Materials (Claiters Prss, Baton Rouge, LA, 1974) pp. 67-75, including discussion.

59. P. Rodriguez, R.W. Armstrong and S.L. Mannan, “The dependence of activation area on grain size in cadmium”, Trans. Ind. Inst. Met., **56**, 189-196 (2003).

60. R.W. Armstrong, “Strength and strain rate sensitivity for nanopolycrystals’, Mechanical Properties of Nanocrystalline Materials, ed, by J.C.M. Li (Pan Stanford Publishing Pte., Ltd., Singapore, 2011) Ch. 3, pp. 61-91.

61. J.F. Bell, “Generalized large deformation behavior for face-centered cubic solids – high purity copper”; Philos. Mag. 10, 107ff (1963); “nickel, aluminum, gold, silver and lead”, Philos., **11**, 1135-1156 (1965).

62. T. Narutani and J. Takamura, “Grain-size strengthening in terms of dislocation density measured by resistivity”, Acta Metall. Mater., **39**, 2037-2049 (1991).

63. P. Rodriguez, “Grain size dependence of the activation parameters for plastic deformation; influence of crysal structure, slip system, and rate-controlling dislocation mechanism”, Metall. Mater. Trans. A, **35A**, 2697-2705 (2004).

64. R.W. Armstrong and P. Rodriguez, “Flow stress/strain rate/grains size coupling for fcc polycrystals”, Philos. Mag., **86**, 5787-5796 (2006).

65. R.J. Asaro and S. Suresh, “Mechanistic models for the activation volume and rate sensitivity in metals with nanocrystalline grains and nano-scale twins”, Acta Mater., **53**, 3369-3382 (2005).

66. G. Weng, “A composite model of nanocrystalline metals”, Mechanical Properties of Nanocrystalline Materials (Pan Stanford Publishing Pte., Ltd., Singapore, 2011) Ch. 4, pp. 94-131.

67. R. Schwaiger, B. Moser, M. Dao. N. Chollacoop and S. Suresh, “Some critical experiments on the strain-rate sensitivity of nanocrystalline nickel”, Acta Mater., **51**, 5159-5172 (2003).

68. R.W. Armstrong, H. Conrad and F.R. N. Nabarro, Mechanical Properties of Nanostructured Materials and Nanocomposites:, ed. by I. Ovid’ko, C.S. Pande, R. Krishnamoorti, E. Lavernia and G. Skandan (Mater. Res. Soc., Warrendale, PA, 2004) **791**, pp. 69-77.

69. T.G. Langdon, “Grain boundary sliding revisited: Developments in sliding over four decades”, J. Mater. Sci., **41**, 597-609 (2006).

70. H. Conrad and J. Narayan, “Mechanism for grain size hardening and softening in Zn”, Acta Mater, **50**, 5067-5078 (2002).

71. J.D. Embury and R.M. Fisher, “The structure and properties of drawn pearlite”, Acta Metall., **14**, 147-152 (1966)

72. J.S.C. Jang and C.C. Koch, “The Hall-Petch relationship in nanocrystalline iron produced by ball milling”, Scr. Metall., **24**, 1599-1604 (1990).

73. D. Jang and M. Atzmon, “Grain size dependence of plastic deformation in nanocrystalline iron”, J. Appl. Phys. **93**, 9282-9286 (2003).

74. G. Purcek, O. Saray, I. Karaman and H.J. Maier, “High strength and high ductility of ultrafine-grained interstitial-free steel produced by ECAE and annealing”, Metall. Mater. Trans. A, **43A**, 1880-1894 (2012).

75. T.R. Smith, R.W. Armstrong, P.M. Hazzledine, R.A. Masumura and C.S. Pande, “Pile-up based Hall-Petch considerations at ultra-fine grain sizes”, Grain Size and Mechanical Properties – Fundamentals and Applications, ed. by M.A. Otooni, R.W. Armstrong, N.J. Grant and K. Ishizaki (Mater. Res. Soc., Pittsburgh, PA, 1995) **362**, pp. 31-37.

76. R.W. Armstrong, “Grain boundary structural influences on nanopolycrystal strength and strain rate sensitivity”, Emerg. Mater. Res., **1**, 31-37 (2012).

77. J.E. Carsley, J. Ning, W.W. Milligan, S.A. Hackney and E.C. Aifantis, “A simple mixtures-based model for the grain size dependence of strength in nanophase metals”, NanoStruct. Mater., **5**, 441-448 (1995).

78. B. Jiang and G.J. Weng, “A generalized self-consistent polycrystal model for the yield strength of nanocrystalline materials”, J. Mech. Phys. Sol., **52**, 1125-1149 (2004).

79. P. Barai and G.J. Weng, “Mechanics of very fine-grained nanocrystalline materials with contributions from grain interior, GB zone, and grain-boundary sliding”, Int. J. Plast., **25**, 2410-2434 (2009).

80. P. Rodriguez and R.W.Armstrong, “Strength and strain rate sensitivity for hcp and fcc nanopolycrystal metals”, (Ind.) Bull. Mater. Sci., **29**, 717-720 (2006).

81. J. Li and G.J. Weng, “A micromechanical approach to the stress – strain relations, strain rate sensitivity and activation volume of nanocrystalline materials”, Int. J. Mech. Mater. Des., **9**, 141-152 (2013).

82. L. Anand, “Polycrystal plasticity”, Mechanics of Materials: Fundamentals and Linkages, ed. by M.A. Meyers, R.W. Armstrong and H. Kirchner (John Wiley and Sons, Inc., N.Y., 1999) Ch. 8, pp. 231-269.

83. H.-K. Kim and S.-I. Oh, “Finite element analysis of grain-by-grain deformation by crystal plasticity with couple stress”, Int. J. Plast., **19**, 1245-1270 (2003).

84. R.W. Armstrong and F.J. Zerilli, “Dislocation mechanics aspects of plastic instability and shear banding”, Mech. Mater., **17**, 319-327 (1994).

85. J.A. Chapman and D.V. Wilson, “The room-temperature ductility of polycrystalline magnesium”, J. Inst. Met., **91**, 39-40 (1962-63).

86. R.W. Armstrong, “Tensile ductility dependence on polycrystal grain size”, Strength of Metals and Alloys; Proc. 7th Int. Conf. ICSMA-CIRMA, ed. by H.J. McQueen, J.-P Bailon, J.I. Dickson, J.J. Jonas and M.G. Akben (Pergamon Press, Oxford, 1985) pp. 195-200.

87. N.J. Petch, “The ductile fracture of polycrystalline alpha-iron”, Philos. Mag., **1**, 186-190 (1956)

88. G.Y. Chin, W.F. Hosford, Jr., and W.A. Backofen, “Ductile fracture of aluminum”, Trans. TMS-AIME, **230**, 437-449 (1964).

89. T.J. Massart and T. Pardoen., “Strain gradient plasticity analysis of the grain-size-dependent strength and ductility of polycrystals with evolving grain boundary confinement”, Acta Mater., **58**, 5768-5781 (2010).

90. C.T. Liu, R.W. Armstrong and J. Gurland, “Determination of the frictional stress for polycrystalline iron and carbon steels from their stress- strain behavior and its grain size dependence”, J. Iron Steel Inst., **209**, 142-146 (1971).

91. X. Zhang, A. Godfrey, X. Huang, N. Hansen and Q. Liu, “Microstructure and strengthening mechanisms in cold-drawn pearlitic steel wire”, Acta Mater., **59**, 3422-3430 (2011).

92. R.W. Armstrong, “60 years of Hall-Petch – past to present nano-scale connections”, Strength of Fine-Grained Metals - 60 Years of Hall-Petch, Univ. Tokyo, 7/16-18/2013, to be printed in a focus issue of the Trans. Japan Inst. Met. (2014).

93. H.C. Sorby, “On the microscopical structure of iron and steel”, J. Iron Steel Inst., [1], 255ff (1887).